recycling

MDPI

Article

Effect of Lead Slag Origin on the Compressive Strength and Immobilization Capacity of Metakaolin-Based Geopolymers

Thiago Vinicius dos Anjos [1], Tarcisio Wolff Leal [2,*], Letícia Maria Scolaro [3], Carlos Itsuo Yamamoto [2], Oscar Khoiti Ueno [1] and Marilena Valadares Folgueras [3]

[1] Northern Plateau Teaching Center (CEPLAN), Department of Production Engineering, State University of Santa Catarina—UDESC, São Bento do Sul 89283-081, SC, Brazil; oscar.ueno@udesc.br (O.K.U.)
[2] Automotive Fuel Analysis Laboratory (LACAUT), Federal University of Paraná—UFPR, Curitiba 81531-980, PR, Brazil; ciyama@ufpr.br
[3] Technological Sciences Center (CCT/PPGCEM), State University of Santa Catarina—UDESC, Joinville 89219-710, SC, Brazil; marilena.folgueras@udesc.br (M.V.F.)
* Correspondence: tarcisio.leal@ufpr.br

Abstract

The use of industrial waste in cementitious materials has been extensively studied as a sustainable alternative to reduce environmental impact and valorize by-products. The aim of this study was to evaluate the effects of the incorporation of secondary lead slag (<200 mesh) from two different sources on the mechanical, microstructural and environmental properties of metakaolin-based geopolymers. After 28 days of curing, analyses of compressive strength, X-ray diffraction, scanning electron microscopy, porosimetry, specific surface area and leaching of potentially toxic elements (PTEs) were performed. The addition of 20% slag led to a reduction in compressive strength of 25.3% (slag A) and 16.7% (slag B) compared to the reference sample. Despite the formation of damaging pores and cracks, both formulations showed effective immobilization of PTEs, with leachate concentrations below the limits specified in NBR 10004 (2004). The results show that the chemical composition of the slag significantly influences the final properties of the material. This study highlights the potential of geopolymers as a solution for the recycling of hazardous waste and the reduction in emissions associated with the cement industry.

Keywords: geopolymer; secondary lead slag; compressive strength; immobilization of potentially toxic elements; sustainability

check for updates

Academic Editors: Simeng Li and Tolulope A. Agunbiade

Received: 28 August 2025
Revised: 17 September 2025
Accepted: 20 September 2025
Published: 28 November 2025

Citation: dos Anjos, T.V.; Wolff Leal, T.; Scolaro, L.M.; Yamamoto, C.I.; Ueno, O.K.; Valadares Folgueras, M. Effect of Lead Slag Origin on the Compressive Strength and Immobilization Capacity of Metakaolin-Based Geopolymers. *Recycling* **2025**, *10*, 215. https://doi.org/10.3390/recycling10060215

Copyright: © 2025 by the authors. Licensee MDPI, Basel, Switzerland. This article is an open access article distributed under the terms and conditions of the Creative Commons Attribution (CC BY) license (https://creativecommons.org/licenses/by/4.0/).

1. Introduction

In view of the climate crisis and growing concerns about greenhouse gases, the construction industry is urgently looking for sustainable alternatives. Geopolymer concrete is a promising solution as it significantly reduces energy consumption (up to 45.8%) and CO_2 emissions (up to 72.4%) compared to Portland cement [1,2]. This is in line with the global decarbonization goals of the Paris Agreement and underlines its potential to contribute to the reduction in CO_2 emissions in the cement and concrete sector, which is responsible for approximately 8% of anthropogenic CO_2 worldwide [3,4].

Beyond sustainability, geopolymers offer valuable properties for construction. These inorganic, amorphous materials have a three-dimensional network of Al–O–Si units formed by the activation of aluminosilicate precursors with alkaline solutions. This process triggers the polymerization of the precursors and leads to a strong and stable network with advantageous structural properties [5–7].

Compressive strength and porosity are two crucial, interrelated properties of geopolymers. The porosity itself depends on the nanopore and micropore structure of the material. Micropores (<2 nm) act as stress concentrators, weakening the material and reducing its compressive strength. Conversely, nanopores (diameter between 2 nm and 50 nm) have a positive influence on mechanical strength. Their ability to efficiently dissipate energy through changes in free volume strengthens the material. Optimizing the ratio of nanopores to micropores in the geopolymer structure is essential for achieving high compressive strength. This optimization can be influenced by factors such as the choice of precursor, the molar ratio of SiO_2/Al_2O_3, and the curing conditions [8].

Another key advantage of geopolymers is their remarkable ability to bind and immobilize potentially toxic elements (PTEs) in their matrix, transforming them from semi-solid waste into stable solid matrices. This property makes them ideal for the treatment and disposal of toxic waste and significantly reduces the risks to the environment and public health [5,9]. The exact mechanism of immobilization is still being researched, but three main processes are thought to be involved [10]: (1) incorporation of ions into the geopolymer network during polymerization; (2) charge balancing, where ions are bound to the structure to neutralize negative charges; (3) physical encapsulation, where precipitates are trapped in the pore system of the material.

Studies have confirmed the effectiveness of metakaolin-based geopolymers in immobilizing various PTEs, including Pb(II), Cd(II), Cu(II), Th(IV) and U(VI) [11,12]. The retention capacity depends on several factors, such as the type of element, the composition of the geopolymer matrix and the production conditions [5]. Beyond this immobilization capacity, recent reviews emphasize that the incorporation of industrial by-products into cementitious systems not only reduces CO_2 emissions (between 23% and 50%, depending on the mixture) but also decreases landfill disposal and the consumption of virgin aggregates [13]. Furthermore, the physical and chemical properties of such residues influence the interfacial transition zone (ITZ), which plays a crucial role in crack formation and long-term durability of composites [14].

Apart from their technical performance, the environmental relevance of geopolymers is also linked to their potential use in the safe disposal of hazardous residues. Contamination of soil and groundwater by PTEs is a major threat to the environment, and lead recycling through secondary smelting contributes significantly to this problem by producing lead slag as a by-product. This slag is rich in pollutants and harmful substances [15], and its composition varies depending on the metals, fluxes and agents used in the smelters, which has a direct impact on the reactions that separate lead from its residues [16].

One promising solution is the inclusion of secondary lead slag in geopolymer production. Research shows that this slag can be effectively integrated into the geopolymer matrix and immobilizes lead and zinc [17]. This approach offers a sustainable alternative for the disposal of toxic waste, reduces the environmental impact and promotes the reuse of materials. Other studies have also investigated the use of molten lead–zinc slags and activated lithium slag as geopolymer precursors, resulting in low porosity matrices with high potential for PTE immobilization [18]. Moreover, the immobilization and solidification of lead smelting slag in fly ash-based geopolymers was reported without significant negative effects on physical properties when slag replacement was limited to 10% [19].

While research has investigated the incorporation of lead slag into geopolymer concrete, a gap in knowledge remains regarding the effects of variations in composition from different sources. Further studies investigating the effects of this variability on the properties and environmental safety of the geopolymer matrix are crucial for optimizing geopolymer production and ensuring its environmental sustainability. Therefore, the aim of this study was to investigate the influence of secondary lead slag waste from two different

sources on the physical, microstructural and environmental properties of metakaolin-based geopolymers. Secondary lead slag was selected because it is abundant as a by-product of battery recycling and there is an urgent need for sustainable and safe applications for this hazardous residue. Its use is also consistent with current concrete practices, where industrial by-products such as fly ash and blast furnace slag are extensively used as SCMs [13]. The slag was used with minimal processing (grinding and sieving), and the program included mechanical, structural and leaching analyses to establish correlations between slag composition and final performance of the geopolymer matrix.

2. Results and Discussion

2.1. Chemical Composition

Chemical composition of metakaolin, slags A and B, NaOH, and Na_2SiO_3, analyzed by XRF, is presented in Table 1. The results are expressed in weight percent.

Table 1. Chemical composition (mass basis) of metakaolin, slag A and B, Na_2SiO_3, and NaOH.

Element	Metakaolin (%)	Slag A (%)	Slag B (%)	Na_2SiO_3 (%)	NaOH (%)
Al	49.47	<loq [1]	7.05	<loq	<loq
Ba	0.46	0.76	<loq	<loq	<loq
Ca	<loq	1.54	2.41	<loq	<loq
Cr	0.03	0.25	1.25	<loq	<loq
Cu	0.02	0.56	0.05	<loq	<loq
Fe	4.00	72.91	71.03	<loq	<loq
H	<loq	<loq	<loq	<loq	2.51
K	3.55	<loq	0.33	<loq	<loq
Mg	2.04	<loq	<loq	<loq	<loq
Mn	<loq	0.49	<loq	<loq	<loq
Na	<loq	<loq	<loq	37.67	57.48
O	<loq	<loq	<loq	39.32	40.00
P	<loq	1.27	<loq	<loq	<loq
Pb	<loq	4.65	1.86	<loq	<loq
S	<loq	13.93	1.84	<loq	<loq
Si	39.21	3.55	14.06	23.01	<loq
Sn	<loq	1.35	<loq	<loq	<loq
Ti	1.21	<loq	<loq	<loq	<loq
Zn	0.01	0.67	0.11	<loq	<loq

[1] Lower than the equipment limit of quantification.

Analysis of the metakaolin composition revealed the presence of aluminum (Al), barium (Ba) and chromium (Cr), elements considered toxic according to NBR 10004 standards [20]. This presence indicates that the leaching of these metals during the leaching test can be partially attributed to metakaolin if they are not present in other components of the mixture. In addition, slag A presented barium (Ba), chromium (Cr) and lead (Pb) in its composition, with a lead content of 4.6%. Slag B, on the other hand, contained aluminum (Al), chromium (Cr) and lead (Pb) and had a lead content of 1.86%. It is important to note that slag A has a significantly higher lead content than slag B. This suggests that the proportion of each slag used in geopolymer production should be adjusted to minimize the leaching of lead from the solid matrix. The presence of heavy metals in metakaolin and slags A and B, therefore, requires attention in the formulation and production of geopolymers. Optimizing the blend composition with a focus on reducing the number of leachable metals is essential to ensure the material's safety and sustainability.

Based on the mass of each component and the final chemical composition, the Si/Al molar ratios were calculated for the specimens produced: 0.90 for GP0, 0.92 for GP20A

and 0.94 for GP20B. These ratios indicate a difference in mechanical properties compared to the geopolymers reported by Duxson et al. [21]. Their study found that geopolymers with a Si/Al ratio of 1.15 had a compressive strength of about 20 MPa and a bimodal pore size distribution characterized by both large, interconnected pores and some degree of crystallinity. To verify this, the compressive strength and pore size distribution of the specimens were measured.

2.2. Compressive Strength

The compressive strengths (CS) of GP0, GP20A and GP20B are shown in Figure 1.

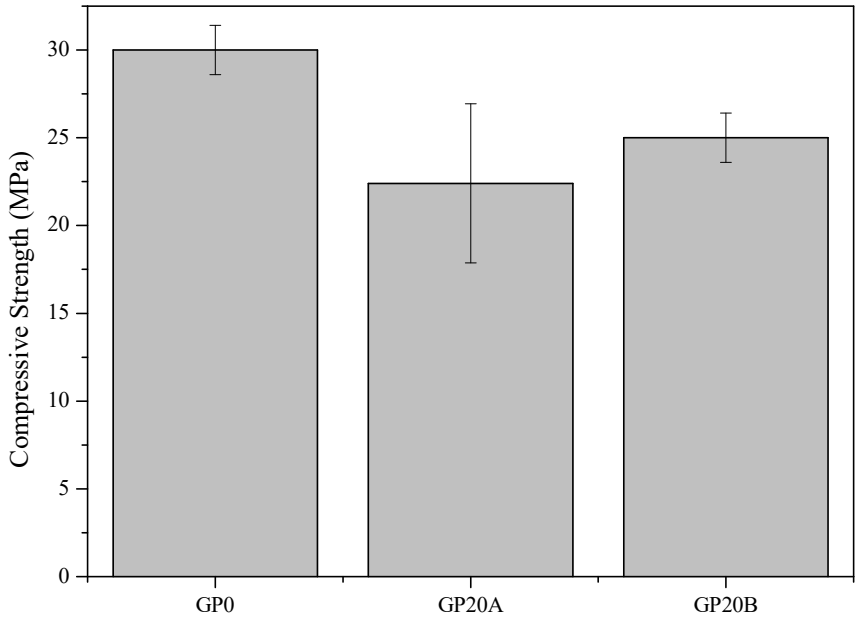


Figure 1. Compressive strength of geopolymerized samples: GP0—standard geopolymer specimen; GP20A—geopolymer specimen with 20% of slag A; GP20B—geopolymer specimen with 20% of slag B.

The samples containing 20% lead slag showed a reduction in CS after 28 days of curing compared to the reference sample (GP0). The reduction was 25.3% for GP20A and 16.7% for GP20B. These results are consistent with studies conducted by Xia et al. [22] and Zhang et al. [23], who observed a decrease in compressive strength when lead slag was added to geopolymeric matrices.

The higher variability observed in the GP20A sample, which is reflected in the higher standard deviation, can be attributed to the soft, fine texture of the slag used. This aligns with the findings of Leong et al. [24], who highlighted the influence of the nature of the precursor on the mechanical strength of geopolymers. They found that the variation in particle size distribution, chemical composition, morphological properties and amorphousness of fly ash significantly affects the CS of geopolymers. Therefore, the soft and fine properties of the slag in the GP20A sample contribute to the higher standard deviation observed, as these factors cause inconsistencies in the geopolymer matrix.

2.3. XRD Analysis

Figure 2 shows the XRD results for samples GP0, GP20A and GP20B; for slags A and B; and for metakaolin. It can be observed that the characteristic crystalline peaks of the quartz phase originating from the metakaolin did not react significantly during geopolymerization in samples GP0, GP20A and GP20B. However, partial dissolution of this phase may have occurred, as reported by Gong et al. [25], where the addition of 5 M NaOH increases the

dissolution of quartz as well as the release of Si, which could contribute to the formation of the geopolymeric gel.

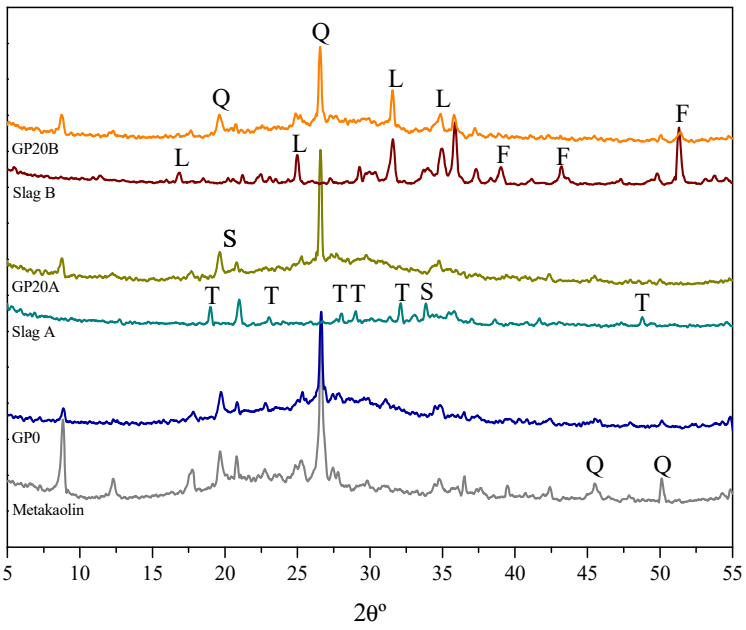


Figure 2. XRD spectra for slags A and B, metakaolin; and for geopolymers GP0, GP20A and GP20B (F: fayalite—Fe_2SiO_4 (01-071-1399); L: lead phosphate—$Pb_8P_2O_{13}$ (00-013-0277); Q: quartz—SiO_2 (00-002-0471); S: sodium aluminum silicate—$NaAlSO_4$ (00-011-0221); T: thenardite—Na_2SO_4 (01-074-2036)).

Slag A exhibited peaks corresponding to sodium sulfate and aluminosilicate phases. However, these phases were absent in GP20A, suggesting that they were dissolved during the geopolymerization process, as only the quartz peaks of metakaolin are visible. One of the factors that could explain the reduction in the mechanical strength of GP20A is the dissolution of sodium sulfate, which reduces the mechanical strength due to a reduced dissolution of aluminosilicate materials. This suggests that the Si content in the hydration products decreases due to a reduction in the pH of the geopolymer, which affects the dissolution of siliceous phases [26].

The effect of Na_2SO_4 is more pronounced in the activation of fly ash, as reported by Criado et al. [27], where the presence of sulfate ions in the solution reduces the rate of alkali activation of fly ash, slows down the formation of N-A-S-H gels and prevents the formation of new compounds. These points may partially explain the reduction in mechanical strength, as no materials have been found in the literature that address the influence of aluminosilicate on the properties of geopolymers.

In slag B, lead phosphate and fayalite phases are present to a considerable extent. In GP20B, the fayalite peaks are not present, indicating the dissolution of this phase in the geopolymer matrix, as reported by Onisei et al. [28], who showed that fayalite is not inert in alkaline environments, and its dissolution depends on the alkalinity of the activating solution and the reactivity of the precursor used. The increase in mechanical strength in GP20B compared to GP20A may be related to the presence of the Fe-containing phase, as reported by Adediran et al. [29], who found that the addition of Fe-rich compounds to the geopolymeric matrix modifies the gels formed, thereby reducing porosity and increasing compressive strength. The lead sulfate phase present in slag B was retained in the GP20B sample, indicating that this phase was not involved in the geopolymerization reactions. It is worth noting that the XRD spectra of the GP20A and GP20B samples, as well as those of slags A and B, are not similar to those observed in the literature.

2.4. Pore Distribution and BET Analyses

Figure 3 shows the specific surface area and pore volume distribution after 28 days of curing, determined by nitrogen adsorption using the Brunauer–Emmett–Teller (BET) and Barrett–Joyner–Halenda (BJH) methods, respectively.

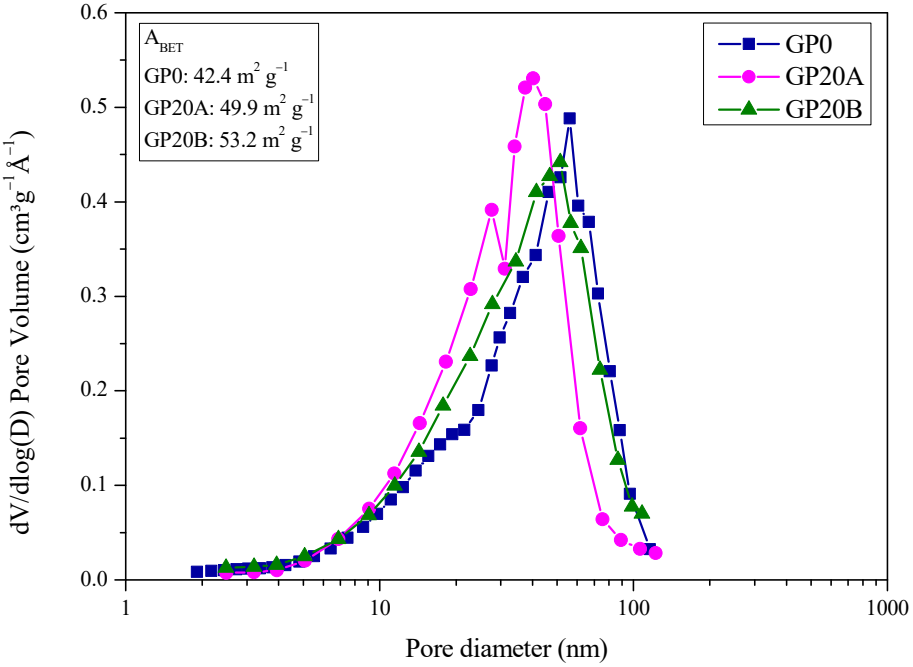
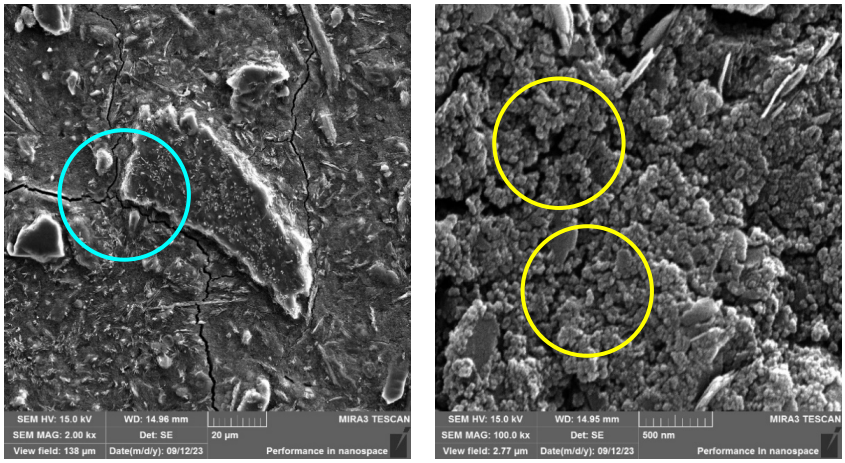


Figure 3. Pore distribution and specific surface area of samples GP0, GP20B and GP20A after 28 days of curing.

The BET results showed that the addition of slags A and B increased the specific surface area of GP20A and GP20B by 17.7% and 25.4%, respectively, compared to GP0. In addition, the pore distribution was also affected by the addition of slags A and B. Compared to the control sample (GP0), both GP20A and GP20B exhibited a reduction in average pore diameter. Specifically, GP20A showed a decrease of 28.13%, while GP20B displayed a slightly lower reduction of 8.25%. These results indicate that the addition of slag decreases the pore size distribution, resulting in smaller pores and consequently larger specific surface areas. This is consistent with the results of Zhang et al. [30], where the addition of Municipal solid waste incineration fly ash (MSWIFA) resulted in a larger specific surface area and refined pore structures. Furthermore, the previously discussed decrease in mechanical strength is consistent with the results presented here. A reduction in pore size is often associated with a loss of mechanical strength, which helps to explain the observed behavior in our samples.

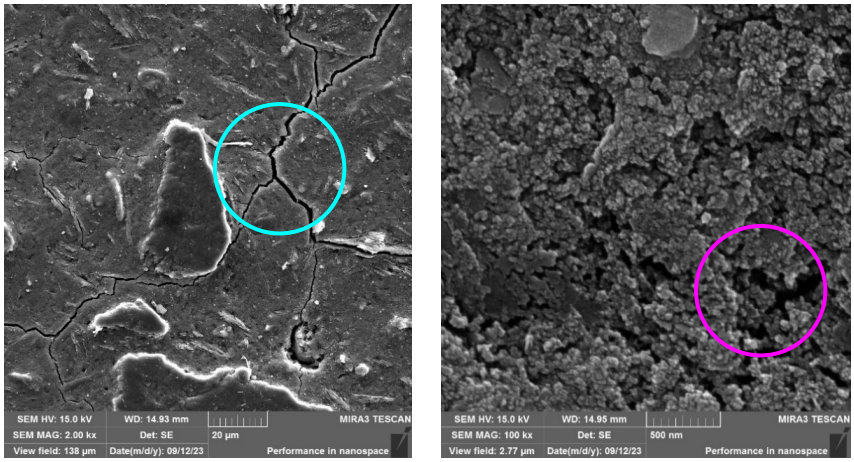
2.5. SEM Quantitative Analysis

Scanning electron microscopy (SEM) was used to evaluate the formation of the geopolymer matrix at magnifications of 2000× and 100,000×. The aim of this analysis was to investigate the influence of the presence of residues on the geopolymer structure. Figures 4–6 show SEM images of the test specimens GP0, GP20A and GP20B, respectively.



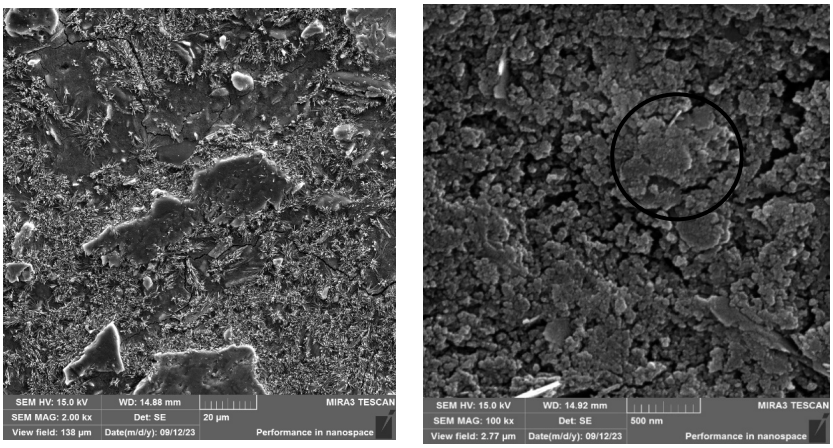
(**a**) (**b**)

Figure 4. SEM images for GP0 specimen: (**a**) 2000× magnification; (**b**) 100,000× magnification (cyan circle: fissure; yellow circle: non-compact matrix).



(**a**) (**b**)

Figure 5. SEM images for GP20A specimen: (**a**) 2000× magnification; (**b**) 100,000× magnification (cyan circle: fissure; magenta circle: harmful pore).



(**a**) (**b**)

Figure 6. SEM images for GP20B specimen: (**a**) 2000× magnification; (**b**) 100,000× magnification (black circle: dense matrix).

The SEM analysis revealed differences in the morphology and compactness of the geopolymer matrix between the samples examined: GP0: At a magnification of 2000×,

the GP0 sample showed a relatively homogeneous matrix with the presence of medium-sized crystals and some surface cracks. However, at higher magnification (100,000×), the matrix appeared less compact, indicating possible weak points within the structure. GP20A: Compared to GP0, the GP20A sample exhibited smaller crystals at 2000× magnification. However, a larger crack was observed, indicating a potential point of vulnerability. At higher magnification (100,000×), the presence of harmful pores was evident, suggesting a possible explanation for a potential reduction in compressive strength observed for this specimen. GP20B: GP20B displayed smaller but profuse crystals at 2000× magnification, along with minor cracks. In contrast to GP0 and GP20A, the SEM image at 100,000× magnification revealed a denser matrix for GP20B. This densification could be attributed to precursor interactions with fayalite, lead phosphate and the higher Si/Al ratio in slag B.

The SEM images qualitatively support the data from the mechanical strength, pore distribution and specific surface area tests as well as the XRD spectra. This strengthens the link between the presence of residues and the final properties of the geopolymer. It was evident that the intrinsic properties of each residue influenced the final quality of the geopolymer. A weaker geopolymer matrix, as observed in sample GP20A, may indicate a lower retention of toxic elements by affecting the immobilization mechanisms of these substances within the geopolymer structure.

2.6. Leaching Analysis

The leaching analysis (Table 2) confirmed successful metal immobilization in GP20A and GP20B (20% slag). Both samples had leachate values below the limits for each toxic element specified in NBR 10004 [20]. This indicates effective encapsulation of the metals in the geopolymer matrix, minimizing their release into the environment. It is important to note that the Ba concentration in the leachate cannot be directly attributed to the residues. This is because Ba is naturally present in metakaolin, a component used in larger quantities in geopolymer formulation. Furthermore, the slightly higher Pb concentration in GP20A compared to GP20B corroborates previous findings regarding the geopolymeric structure of this sample. In addition, a solubility analysis should be conducted to verify the inertization of the toxic elements in the geopolymer structure.

Table 2. Leaching analysis results for GP0, GP20A and GP20B specimens (results in mg L^{-1}).

Element	GP0	GP20A	GP20B	NBR 10004:2004 Standard Limit
Ag	<0.05	<0.05	<0.05	5
As	<0.01	<0.01	<0.01	1
Ba	2.57 ± 0.05	1.88 ± 0.03	5.42 ± 0.06	70
Cd	<0.005	<0.005	<0.005	0.5
Cr	<0.025	<0.025	<0.025	5
Hg	<0.01	<0.01	<0.01	0.1
Pb	<0.005	0.85 ± 0.04	0.58 ± 0.05	1
Se	<0.005	<0.005	<0.005	1

3. Experimental

3.1. Secondary Lead Slag Pre-Treatment

Secondary lead slag obtained from two different companies was used for this study. Slag A (Figure 7a), supplied by Company A (Acumuladores Moura S/A, Modelo, Brazil), came from a pyrometallurgical process. This process used pig iron and sodium carbonate. Sodium carbonate lowered the melting point of the lead and facilitated the treatment of the sulfur gases from acid batteries. Despite its benefits, this process produced a slag

with a soft, powdery texture. Slag B (Figure 7b), on the other hand, came from Company B (Pindorama, Brazil) and was produced using a similar pyrometallurgical process, but without the addition of sodium carbonate. This slag had a high hardness, which made it exceedingly difficult to grind. For the pre-treatment, each slag was crushed in a planetary mill (Servitech, CT 241, Tubarão, Brazil) and then passed through a fine sieve (200 mesh).



(**a**) (**b**)

Figure 7. Secondary lead slags: (**a**) slag A and (**b**) slag B.

3.2. Preparation of Specimens

Metakaolin from Metacaulim do Brasil and secondary lead slags were used as precursors to produce geopolymers. The alkaline activator was prepared by dissolving granular sodium hydroxide (NaOH) and sodium silicate (Na_2SiO_3) in water to obtain a solution containing 5 M NaOH and 1.6 M Na_2SiO_3, which was subsequently combined with metakaolin in a 1:1 weight ratio for all formulations. Three types of test specimens were prepared: one reference without slag (GP0) and two with 20 wt% slag (GP20A and GP20B). The 20 wt% substitution level was chosen based on preliminary laboratory tests, which indicated suitable processability and mechanical performance and matched the optimal ranges reported by Li et al. [17] for similar systems. After mixing, the pastes were manually stirred, poured into PVC molds (1 inch diameter and 2 inches high) and vibrated to release entrapped air. The specimens were then cured at room temperature for approximately 96 h, demolded and stored until testing after 28 days of curing (Figure 8).



(**a**) (**b**)

Figure 8. Geopolymer specimens prepared with 20 wt% of slag A (**a**) and slag B (**b**).

3.3. Chemical Composition of Precursors

Before characterizing the specimens, a chemical composition analysis was conducted to evaluate the elements present in each component separately. This ensures that the elements from the slags are correctly attributed during the leaching test. The chemical

composition was determined using a SHIMADZU EDX 720 X-ray Fluorescence (XRF) instrument (Shimadzu Corporation, Kyoto, Japan).

3.4. Characterization of Specimens and Precursors

After the curing period, the test specimens and their precursors were subjected to a series of characterizations to evaluate the influence of the addition of residues on the chemical and structural quality of the geopolymers. The following techniques were employed: (1) Compressive Strength Tests: compressive strength was tested using an EMIC Universal Mechanical Testing Machine (model DL30000, Emic, São José dos Pinhais, Brazil) at a loading rate of 0.05 mm s^{-1} and a load capacity of 100 MPa. (2) Surface Area and Porosity Analysis: the ASAP 2020 PLUS instrument from Micromeritics (Norcross, GA, USA) was used to determine the surface area and porosity of the samples; (3) X-ray Diffraction (XRD): a SHIMADZU model 6000 X-ray diffractometer (Shimadzu Corporation, Kyoto, Japan) was used to identify crystalline phases. The samples were scanned between 5° and 55° (2-theta) at a scan speed of 2° min^{-1}. (4) Scanning Electron Microscopy (SEM): the morphology of the samples was examined using a Tescan scanning electron microscope (model Mira 3, TESCAN, Brno, Czech Republic). To prepare the samples, they were embedded in epoxy resin, polished, cleaned and finally coated with a thin gold film. (5) Leaching Tests: the leaching behavior was evaluated according to the standard NBR 10005 [31] or the US EPA SW-846 method 1311 [32]. The leachate was then analyzed for several elements using a VARIAN ICP-720ES instrument (Agilent, Palo Alto, CA, USA).

4. Conclusions

This study showed that the addition of 20% by weight of secondary lead slag from two sources to metakaolin-based geopolymers directly affects their performance. GP20A showed a 25.3% reduction in compressive strength, while GP20B showed a smaller decrease of 16.7%, due to the higher Si and Fe content, which favors better compaction of the matrix. Microstructural analyses confirmed that the slag composition influenced pore distribution, gel formation and crack development: slag A promoted the formation of damaging pores, while slag B contributed to a denser matrix. Despite having lower strength, both slag-containing geopolymers effectively immobilized Pb, Cd, Cr and Ba, with leachate levels below the limits set by NBR 10004 (2004), confirming their environmental compatibility. The study was limited to a single substitution level. Aspects of durability such as resistance to freeze–thaw cycles, carbonation and long-term leaching were not investigated. Future work should investigate different incorporation levels, pre-treatment strategies to reduce pore formation and long-term durability to improve the applicability of these materials in practice. Overall, the results underline the potential of geopolymers as sustainable binders for waste recycling and CO_2 reduction. At the same time, they emphasize the need for further research to improve structural performance and durability, as the properties of the waste—and consequently the quality of the geopolymer—depend directly on the process from which the residue originates.

Author Contributions: Conceptualization, O.K.U. and M.V.F.; methodology, L.M.S. and T.W.L.; software, T.W.L.; validation, L.M.S. and T.W.L.; formal analysis, T.W.L.; investigation, T.V.d.A.; resources, M.V.F.; data curation, T.V.d.A.; writing—original draft preparation, T.V.d.A. and T.W.L.; writing—review and editing, T.W.L., L.M.S. and C.I.Y.; visualization, T.W.L.; supervision, O.K.U. and M.V.F.; project administration, M.V.F.; funding acquisition, M.V.F. All authors have read and agreed to the published version of the manuscript.

Funding: This research received no external funding.

Data Availability Statement: The data presented in this study are available on request from the corresponding author due to the absence of a centralized repository, as the datasets were produced and retained individually by the contributing authors.

Acknowledgments: The authors are grateful for the infrastructure provided by the Multi-User Facility of the Center for Technological Sciences of the State University's Technological Sciences Center; C-LabMu of State University of Ponta Grossa; and the Research Foundation of Santa Catarina (FAPESC).

Conflicts of Interest: The authors declare that they have no known competing financial interests or personal relationships that could have appeared to influence the work reported in this paper.

Abbreviations

The following abbreviations are used in this manuscript:

BET	Brunauer–Emmett–Teller
BJH	Barrett–Joyner–Halenda
CS	Compressive Strength
EPA	Environmental Protection Agency (United States)
ICP-OES	Inductively Coupled Plasma Optical Emission Spectrometry
NBR	Norma Brasileira (Brazilian Standard)
SEM	Scanning Electron Microscopy
XRD	X-ray Diffraction
XRF	X-ray Fluorescence

References

1. Borges, P.H.R.; Lourenço, T.M.d.F.; Foureaux, A.F.S.; Pacheco, L.S. Estudo Comparativo Da Análise de Ciclo de Vida de Concretos Geopoliméricos e de Concretos à Base de Cimento Portland Composto (CP II). *Ambiente Construído* **2014**, *14*, 153–168. [CrossRef]
2. Gomes, K.C.; Carvalho, M.; Diniz, D.d.P.; Abrantes, R.d.C.C.; Branco, M.A.; Carvalho Junior, P.R.O.d. Carbon Emissions Associated with Two Types of Foundations: CP-II Portland Cement-Based Composite vs. Geopolymer Concrete. *Matéria* **2019**, *24*, 1–10. [CrossRef]
3. Farfan, J.; Fasihi, M.; Breyer, C. Trends in the Global Cement Industry and Opportunities for Long-Term Sustainable CCU Potential for Power-to-X. *J. Clean. Prod.* **2019**, *217*, 821–835. [CrossRef]
4. Summerbell, D.L.; Barlow, C.Y.; Cullen, J.M. Potential Reduction of Carbon Emissions by Performance Improvement: A Cement Industry Case Study. *J. Clean. Prod.* **2016**, *135*, 1327–1339. [CrossRef]
5. Davidovits, J. Properties of Geopolymer Cements. In Proceedings of the First International Conference on Alkaline Cements and Concretes, Kiev, Ukraine, 11–14 October 1994; pp. 131–149.
6. Jindal, B.B.; Alomayri, T.; Hasan, A.; Kaze, C.R. Geopolymer Concrete with Metakaolin for Sustainability: A Comprehensive Review on Raw Material's Properties, Synthesis, Performance, and Potential Application. *Environ. Sci. Pollut. Res.* **2022**, *30*, 25299–25324. [CrossRef]
7. Khale, D.; Chaudhary, R. Mechanism of Geopolymerization and Factors Influencing Its Development: A Review. *J. Mater. Sci.* **2007**, *42*, 729–746. [CrossRef]
8. Akono, A.T.; Koric, S.; Kriven, W.M. Influence of Pore Structure on the Strength Behavior of Particle- and Fiber-Reinforced Metakaolin-Based Geopolymer Composites. *Cem. Concr. Compos.* **2019**, *104*, 103361. [CrossRef]
9. Shi, C.; Fernández-Jiménez, A. Stabilization/Solidification of Hazardous and Radioactive Wastes with Alkali-Activated Cements. *J. Hazard. Mater.* **2006**, *137*, 1656–1663. [CrossRef] [PubMed]
10. Zhang, X.L.; Yao, A.L.; Chen, L. A Review on the Immobilization of Heavy Metals with Geopolymers. *Adv. Mat. Res.* **2013**, *634–638*, 173–177. [CrossRef]
11. Fan, J.; Yan, J.; Zhou, M.; Xu, Y.; Lu, Y.; Duan, P.; Zhu, Y.; Zhang, Z.; Li, W.; Wang, A.; et al. Heavy Metals Immobilization of Ternary Geopolymer Based on Nickel Slag, Lithium Slag and Metakaolin. *J. Hazard. Mater.* **2023**, *453*, 131380. [CrossRef]
12. Li, S.; Huang, X.; Muhammad, F.; Yu, L.; Xia, M.; Zhao, J.; Jiao, B.; Shiau, Y.; Li, D. Waste Solidification/Stabilization of Lead–Zinc Slag by Utilizing Fly Ash Based Geopolymers. *RSC Adv.* **2018**, *8*, 32956–32965. [CrossRef]
13. Newton-Hoare, L.; Jamieson, S.; White, G. Review of the Use of Waste Materials in Rigid Airport Pavements: Opportunities, Benefits and Implementation. *Sustainability* **2025**, *17*, 6959. [CrossRef]

14. Golewski, G.L. The Investigation of Shear Fracture Toughness and Structure of ITZ of Limestone Concrete with Different Aggregate Grain Size. *Materials* **2025**, *18*, 3954. [CrossRef]
15. Griggio, R.C.; Luvizão, G. Avaliação Das Características Químicas, Volumétricas e Mecânicas, Quando Incorporado Escória de Chumbo Proveniente Da Reciclagem de Baterias. *Conhecimento Em Construção* **2021**, *8*, 61–78.
16. Santacruz Torres, J.; Torres Agredo, J. Aprovechamiento de Escorias de Fundición Secundaria de Plomo En Ladrillos Cerámicos. *Cienc. E Ing. Neogranadina* **2019**, *29*, 7–18. [CrossRef]
17. Li, J.; Liu, Y.; Ke, X.; Jiao, X.; Li, R.; Shi, C. Geopolymer Synthesized from Electrolytic Manganese Residue and Lead-Zinc Smelting Slag: Compressive Strength and Heavy Metal Immobilization. *Cem. Concr. Compos.* **2022**, *134*, 104806. [CrossRef]
18. Dai, B.-B.; Zou, Y.; He, Y.; Lan, M.; Kang, Q. Solidification Experiment of Lithium-Slag and Fine-Tailings Based Geopolymers. *Sustainability* **2023**, *15*, 4523. [CrossRef]
19. Ogundiran, M.B.; Nugteren, H.W.; Witkamp, G.J. Immobilisation of Lead Smelting Slag within Spent Aluminate—Fly Ash Based Geopolymers. *J. Hazard. Mater.* **2013**, *248–249*, 29–36. [CrossRef]
20. *NBR 10004*; Resíduos Sólidos—Classificação. Associação Brasileira de Normas Técnicas (ABNT): Rio de Janeiro, Brazil, 2004.
21. Duxson, P.; Provis, J.L.; Lukey, G.C.; Mallicoat, S.W.; Kriven, W.M.; Van Deventer, J.S.J. Understanding the Relationship between Geopolymer Composition, Microstructure and Mechanical Properties. *Colloids Surf. A Physicochem. Eng. Asp.* **2005**, *269*, 47–58. [CrossRef]
22. Xia, M.; Muhammad, F.; Zeng, L.; Li, S.; Huang, X.; Jiao, B.; Shiau, Y.C.; Li, D. Solidification/Stabilization of Lead-Zinc Smelting Slag in Composite Based Geopolymer. *J. Clean. Prod.* **2019**, *209*, 1206–1215. [CrossRef]
23. Zhang, Q.; Cao, X.; Sun, S.; Yang, W.; Fang, L.; Ma, R.; Lin, C.; Li, H. Lead Zinc Slag-Based Geopolymer: Demonstration of Heavy Metal Solidification Mechanism from the New Perspectives of Electronegativity and Ion Potential. *Environ. Pollut.* **2022**, *293*, 118509. [CrossRef]
24. Leong, H.Y.; Ong, D.E.L.; Sanjayan, J.G.; Nazari, A. Suitability of Sarawak and Gladstone Fly Ash to Produce Geopolymers: A Physical, Chemical, Mechanical, Mineralogical and Microstructural Analysis. *Ceram. Int.* **2016**, *42*, 9613–9620. [CrossRef]
25. Gong, K.; Aytas, T.; Zhang, S.Y.; Olivetti, E.A. Data-Driven Prediction of Quartz Dissolution Rates at Near-Neutral and Alkaline Environments. *Front. Mater.* **2022**, *9*, 1–15. [CrossRef]
26. Ma, C.; Zhao, B.; Wang, L.; Long, G.; Xie, Y. Clean and Low-Alkalinity One-Part Geopolymeric Cement: Effects of Sodium Sulfate on Microstructure and Properties. *J. Clean. Prod.* **2020**, *252*, 119279. [CrossRef]
27. Criado, M.; Jiménez, A.F.; Palomo, A. Effect of Sodium Sulfate on the Alkali Activation of Fly Ash. *Cem. Concr. Compos.* **2010**, *32*, 589–594. [CrossRef]
28. Onisei, S.; Lesage, K.; Blanpain, B.; Pontikes, Y. Early Age Microstructural Transformations of an Inorganic Polymer Made of Fayalite Slag. *J. Am. Ceram. Soc.* **2015**, *98*, 2269–2277. [CrossRef]
29. Adediran, A.; Yliniemi, J.; Carvelli, V.; Adesanya, E.; Illikainen, M. Durability of Alkali-Activated Fe-Rich Fayalite Slag-Based Mortars Subjected to Different Environmental Conditions. *Cem. Concr. Res.* **2022**, *162*, 106984. [CrossRef]
30. Zhang, P.; Han, X.; Guo, J.; Zhang, H. Fractal Characteristics of Geopolymer Mortar Containing Municipal Solid Waste Incineration Fly Ash and Its Correlations to Pore Structure and Strength. *Fractal Fract.* **2022**, *6*, 676. [CrossRef]
31. *NBR 10005*; Lixiviação de Resíduos—Procedimento. Associação Brasileira de Normas Técnicas (ABNT): Rio de Janeiro, Brazil, 2004.
32. *SW-846 Test Method 1311*; Toxicity Characteristic Leaching Procedure. U.S. Environmental Protection Agency (US EPA): Washington, DC, USA, 1992.

Disclaimer/Publisher's Note: The statements, opinions and data contained in all publications are solely those of the individual author(s) and contributor(s) and not of MDPI and/or the editor(s). MDPI and/or the editor(s) disclaim responsibility for any injury to people or property resulting from any ideas, methods, instructions or products referred to in the content.